The object of this study is to regulate charge and discharge currents in battery systems and its affect on thermal behavior under dynamic battery operating conditions. The problem to be solved is the development of battery management framework which accounts for charging current regulation and a load shedding mechanism for discharge current regulation for temperature and voltage control of battery bank.

Simulation results demonstrate that the proposed hybrid framework for the battery control system maintains stable temperature levels during both charging and discharging cycles, where during charging the current is regulated based on terminal voltage, temperature and rate of change of temperature, while during discharging control is based on temperature and rate of change of both temperature rise and voltage drop.

The distinctive feature of the proposed framework is the hybrid control structure that applies different regulation strategies for charging and discharging processes by using fuzzy logic controllers. In this approach, fuzzy logic adjusts the charging current according to the state of charge, voltage, and temperature of the battery cells, at the same time load shedding and load transfer regulate the discharge current to maintain safe operating conditions.

The proposed system was simulated in MATLAB with 3 charge–discharge cycles. It maintained temperature within 45°C setpoint with minimal overshoot and voltage drop amount not more than 25% nominal battery bank voltage.

The results can be applied to the development of battery management systems for battery banks in energy storage, electrical vehicles, essential power supplies in industrial applications, and solar/wind power generation system

Keywords: battery temperature regulation, charging fuzzy logic control, discharge by load shedding

UDC 621.355:62-50:004.8
DOI: 10.15587/1729-4061.2026.358679

DEVELOPMENT OF BATTERY CHARGING-DISCHARGING CURRENT REGULATION STRATEGY BY USING FUZZY LOGIC CONTROLLERS

Rahim Mammadzada
Corresponding author
PhD Candidate*
E-mail: rahim.mammadzada02@gmail.com
ORCID: https://orcid.org/0009-0008-7552-2790
Ruslan Mammadov
PhD Candidate*
ORCID: https://orcid.org/0009-0003-8723-639X
*Department of Instrumentation Engineering
Azerbaijan State Oil and Industry University (ASOIU)
Azadliq ave., 34, Baku, Azerbaijan, AZ 1010

Received 28.01.2026
Received in revised form 06.03.2026
Accepted date 15.04.2026
Published date 30.04.2026

How to Cite: *Mammadzada, R., Mammadov, R. (2026). Development of battery charging-discharging current regulation strategy by using fuzzy logic controllers. Eastern-European Journal of Enterprise Technologies, 2 (2 (140)), 111–126. https://doi.org/10.15587/1729-4061.2026.358679*

1. Introduction

In recent years, electrochemical energy storage systems have become a main component of modern electrical power distribution, including renewable energy integration and distributed storage systems. Higher energy density, compact architectures, longer lifetime, fast-charging capability, environmentally friendly batteries are important for modern energy storage systems. In modern conditions, batteries are frequently subjected to high current loads, rapid cycling, and elevated thermal stress. As a result, thermal behavior has emerged as a critical factor influencing safety, reliability, lifetime, and overall system performance. Failures related to overheating and thermal runaway continue to cause serious technical and economic risks, particularly in large-scale and high-power applications.

Heat generation in lithium-ion cells arises from electrochemical heating, which directly depend on current magnitude. Thus, temperature cannot be effectively controlled without structured current management. Moreover, temperature variations influence internal resistance, voltage characteristics, ageing rate, and state-of-charge estimation accuracy. In modern battery applications, where high C-rate charging and discharging are common, this can lead to acceleration of degradation and reduced operational reliability and safety.

The impotency of further study is also reinforced by the bidirectional current flow nature of battery operation. Charging and discharging processes of the batteries present fundamentally different constraints and control opportunities. During discharge and charging, the current is actively regulated by the battery management system (BMS), and excessive temperature rise represents a major safety and reliability concern. These characteristics indicate that advanced automatic thermal protection strategies may be required for modern battery systems. These advanced practical approaches improve operational safety, reliability, extend battery lifetime, reduce degradation-related costs. Advanced battery electro-thermal control strategies can enable more efficient usage of battery capacity while preventing localized overheating and thermal imbalance.

2. Literature review and problem statement

In paper [1], a fuzzy controller optimized by genetic algorithm for lithium-ion battery charging is proposed. Here, the charging current is regulated based on temperature using ECM (equivalent circuit model). The objective of this work was to reduce the charging time while regulating battery temperature. However, this work focuses on charging with fuzzy rule optimization, with discharging being not considered.

In paper [2], a fuzzy BMS (battery management system) for charging and cell balancing is proposed. This approach supports hardware integration and demonstrates high adapt-

ability with other battery chemistries by membership function adjustments. However, the control strategy remains mainly focused on charging and balancing, while the integration of discharging is not clearly addressed.

In paper [3], the thermal and electrical behavior of solar panels, converters and battery storage systems of a DC-DC microgrid is analyzed. This work emphasizes how irradiance and temperature changes propagate across generation, conversion and storage components of a DC-DC microgrid. Although this work is mainly conceptual, it does show the importance of BMS algorithms for battery charging and discharging, as solar panel's power output fluctuations could require discharging at any given time.

In paper [4], a fuzzy-PID controller optimized by modified slime mold algorithm is proposed for battery management in photovoltaic microgrids. In this work, SOC and voltage data is used to tune PID gains and fuzzy rules for charging and discharging operations under varying loads. However, temperature of the battery is not taken into considered.

In paper [5], a prediction method for remaining charge time estimation is proposed. This method is based on electro-thermal model to capture temperature dynamics based on ambient temperature, thermal management and internal heating. This approach demonstrates high prediction accuracy for −20°C to 45°C temperatures through electro-thermal interactions. In [6], an adaptive neuro-fuzzy inference system (ANFIS) approach to predict future battery temperature is proposed. In this work, real-time measurements of internal resistance and open circuit voltage increase the prediction accuracy. This method demonstrates short-term temperature prediction across different battery chemistries and ambient conditions. However, both of these works do not directly provide actionable strategies for limiting heat generation.

In paper [7], a fast-charging predictive thermal management strategy for electric vehicles is proposed. In this work, nonlinear model predictive control is combined with offline programming to regulate two phase cooling components like pump, compressor and heaters to prevent overheating. While this approach offers improved energy efficiency at moderate temperatures with more efficient thermal regulation, it does not account for sudden load shedding or transferring affects during discharge.

In paper [8], an adaptive fuzzy control strategy for multilayer battery equalization is proposed. Here, the equalization current changes based on the state of charge (SOC) and temperature as key inputs. This results in faster energy transfer between cells and improved thermal management during balancing. While this method does provide better equalization time and lower temperature than convectional buck-boost methods, it also assumes constant current during discharging.

In paper [9] a fuzzy logic-controlled heating system for the electromotive vehicles is proposed. This work demonstrates more efficient use of heater which in its turn helps the vehicle to achieve more travel distance. However, this work uses external heater and considers it as a standalone external heating system, which although efficient, will not account for thermal runaway prevention.

In paper [10] two separate fuzzy logic control strategies for charging and discharging are proposed. The fuzzy FLC for charging considers rate of change of current and voltage as its input parameters, while the FLC for discharging considers voltage and current. However, the temperature is not considered as an input parameter in either of the FLC controllers and this works overall structure can only support battery banks with eight cells at most.

From this analysis, several local problems have been identified:

– battery temperature control is mainly applied for charging [1, 2];

– in PV microgrids, battery temperature control is often overlooked [3, 4];

– battery temperature control is also mainly predicted for charging [5–7];

– even when discharge is considered, most works assume constant current for discharging [6, 8], or in other cases, either consider temperature consideration as standalone external control systems [9], or don't include temperature [10].

The general unresolved problem emerging from these studies is advanced fuzzy logic-based temperature control system should adopt method for real-time, temperature-based battery management for charging and discharging.

3. The aim and objectives of the study

The aim of the study is to develop a unified control framework for charge and discharge current regulation in battery banks through the integration of fuzzy logic charging control, load shedding and load transferring-based discharge control. This will allow to stabilize battery temperature, regulate current flow during charging and discharging cycles, and improve the operational reliability, safety and performance of batteries.

To achieve the aim, the following objectives were set:

– to setup Simulation environment for the battery bank in MATLAB;

– to design a charging current regulation strategy with fuzzy logic control algorithm, which accounts voltage, temperature and rate of change of temperature;

– to design a structured load shedding and load transferring algorithm for discharge current control;

– to evaluate its effectiveness in terms of current regulation and temperature stabilization.

4. Materials and methods

4. 1. The object and hypothesis of the study

The object of this study is to regulate charge and discharge currents in battery systems and its affect on thermal behavior under dynamic battery operating conditions.

The main study hypothesis is that the integration of fuzzy logic control for charging current regulation and load shedding for discharge current management within a battery management framework can improve temperature stabilization and current regulation compared to conventional monitoring-only strategy approaches [11].

The study adopts the following assumptions. The battery pack consists of serially connected cells that operate under ideal, identical environmental conditions. Each battery cell is represented using an equivalent circuit model with a voltage source and internal resistance, and the thermal behavior of the cells is represented through a lumped thermal mass connected to the electrical model through a thermal port.

Simplifications were also made to keep the study practicable. The battery pack is modelled using a predefined table-based battery model available in the Simscape Electrical

library. Thermal interactions between cells are simplified using a lumped thermal representation, and the control strategies are evaluated within a simulation environment without hardware implementation.

4. 2. General block diagram of battery management system

The general block diagram of battery bank charging and discharging is shown in Fig. 1. The black solid lines represent the main electrical power circuit. The green dashed lines indicate the connections of the voltage transducer (VT) and current transducer (CT) for battery bank voltage and current measurement to the battery management system (BMS). The blue dashed lines represent the load switch binary control signal from the BMS. The yellow dashed line shows the analogue control signal from the BMS to the charger. The orange dashed lines represent the key parameters measurement and transmitting to the BMS, including the single battery voltage, internal resistance, state of charge (SoC), and temperature for each cell.

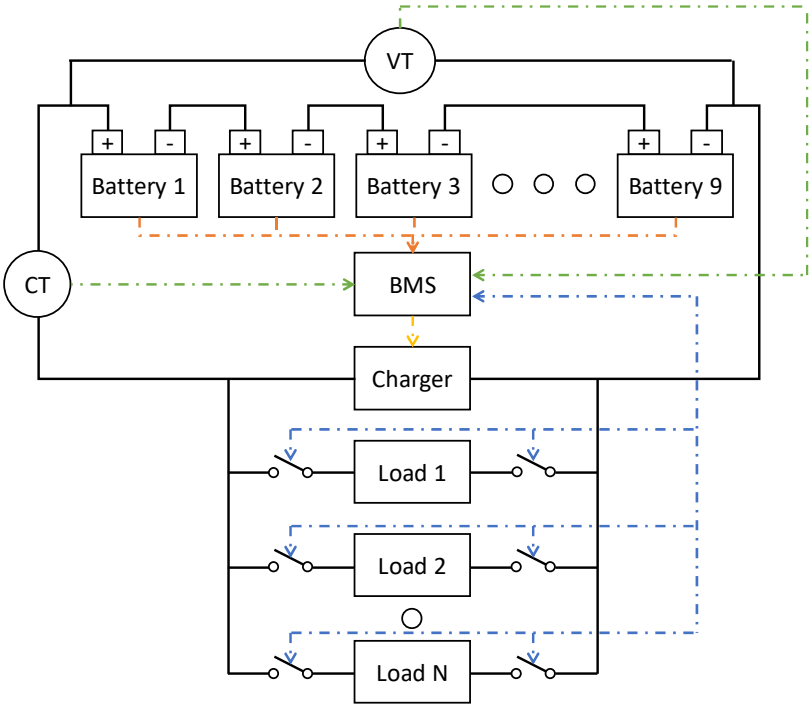

Fig. 1. General block diagram of battery charge-discharge system

For this work, a cell count of 9 was selected; this approach is true for any number of serially connected battery bank configurations.

4. 3. Battery bank electrical domain modelling

Lithium-ion batteries are commonly represented using equivalent circuit models (ECMs), which balance physical accuracy and computational efficiency. In these models, the battery is described by a network of resistors and capacitors that reproduce its electrical response under load. The series resistance R0 captures the instantaneous voltage drop, while one or more RC branches represent transient relaxation effects over short and long-time scales, as shown in Fig. 2.

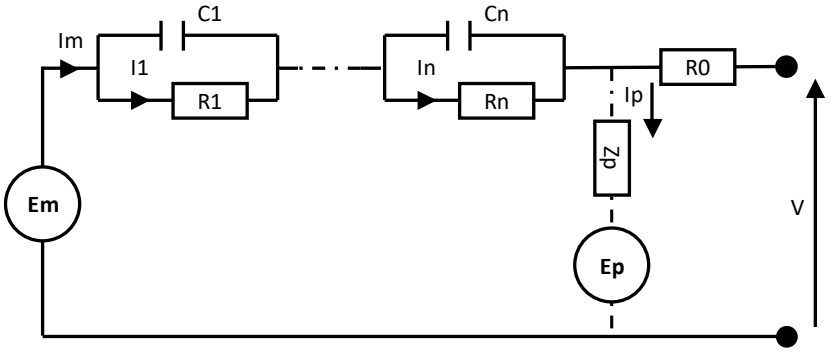

Fig. 2. Equivalent circuit model of batteries

Accurate voltage prediction requires proper parameterization of these RC branches under varying operating conditions. This is typically achieved using lookup tables that relate state-of-charge (SoC) and temperature to internal parameters. As SoC decreases, internal resistance increases while effective capacitance decreases, reflecting reduced charge storage capability. Temperature further influences performance: low temperatures increase resistance and limit available capacity, whereas higher temperatures reduce resistance but accelerate degradation mechanisms.

Software environments such as MATLAB provide libraries with prebuilt, table-based battery models that incorporate these dependencies and enable coupled electrical and thermal simulations [12]. However, despite this modelling capability, establishing a clear linkage between cell-level measurements and battery bank-level control decisions within a complete battery management system remains a challenge.

4. 4. Battery bank thermal domain modelling

In addition to electrical behavior, the thermal behavior of battery cells must be considered. In this work, it is possible to consider only a two-dimensional arrangement, with cells organized in rows and columns, as shown in Fig. 3. The position of cells within the pack determines which surfaces are exposed for heat dissipation. Corner cells are exposed on two side faces and the top surface, side cells on one side face and the top surface, and central cells only on the top surface. In a full three-dimensional pack, all surfaces of cells below the top layer would be blocked by the cells above, leaving only the top layer exposed for heat transfer.

This work considers an engineering study of a battery bank consisting of nine Valence U27-12X batteries connected in series in a single 3 × 3 layer. In addition to the dimensions and surface areas, it is important to account for the air exposure and contact of cells for accurate thermal modelling, as shown in Fig. 4.

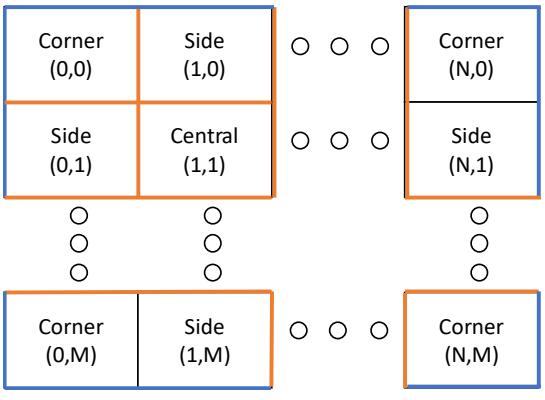

Fig. 3. General block diagram of single-layered battery alignment

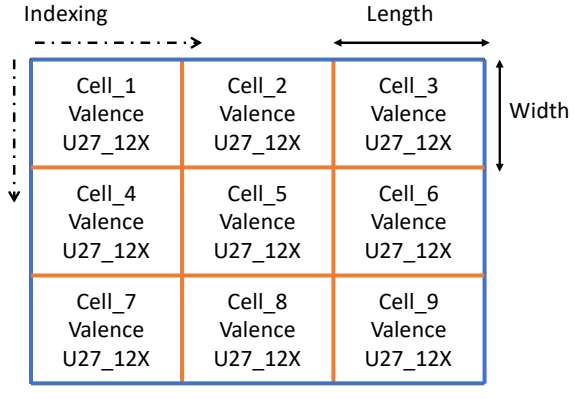

Fig. 4. Block diagram of 3 × 3 single layered battery alignment

Table 1 lists the dimensions and surface areas of each side of a Valence U27-12X cell. Table 2 summarizes the number of exposed sides for each cell and the resulting total air-exposed and contact areas within the battery bank. For this study, the bottom face of each cell is considered thermally isolated.

Table 1

Dimensional parameter of the valence U27_12X

Parameter	Symbol	Value
Length	L	0.306 m
Width	W	0.172 m
Height	H	0.225 m
Length Side	A_{LH}	0.06885 m^2
Width Side	A_{WH}	0.03870 m^2
Top Face	A_{LW}	0.05263 m^2

When battery modules are in direct contact, heat is transferred between neighboring cells through their casings. The transfer path includes conduction through the first module's casing, the thermal contact resistance at the interface, and conduction through the adjacent module's casing. For steady-state conduction through a flat layer, the thermal resistance is defined as

$$R_{Case} = \frac{t_{Case}}{k_{Case} A}, \quad (1)$$

where t – the material thickness, k – the thermal conductivity, and A – the heat transfer area. Thermal contact resistance is commonly reported in an area-normalized form $R''_{Contact}$ which can be converted into standard thermal resistance as

$$R_{Contact} = \frac{R''_{Contact}}{A}. \quad (2)$$

Table 2

Each cells exposer and contact area based on their placement

Cell ID	Air exposed face count			Total exposer area	In contact face count			Total contact area
	A_{LH}	A_{WH}	A_{LW}	$A_{Exposer}$	A_{LH}	A_{WH}	A_{LW}	$A_{Contact}$
Cell 1	1	1	1	0.16018 m^2	1	1	0	0.10755 m^2
Cell 2	0	1	1	0.09133 m^2	2	1	0	0.1764 m^2
Cell 3	1	1	1	0.16018 m^2	1	1	0	0.10755 m^2
Cell 4	1	0	1	0.12148 m^2	1	2	0	0.14625 m^2
Cell 5	0	0	1	0.05263 m^2	2	2	0	0.2151 m^2
Cell 6	1	0	1	0.12148 m^2	1	2	0	0.14625 m^2
Cell 7	1	1	1	0.16018 m^2	1	1	0	0.10755 m^2
Cell 8	0	1	1	0.09133 m^2	2	1	0	0.1764 m^2
Cell 9	1	1	1	0.16018 m^2	1	1	0	0.10755 m^2

For two identical battery modules in contact, heat must pass through two casing layers and the interface between them. Substituting the corresponding resistances yields the overall thermal resistance between adjacent modules

$$R_{Total} = 2R_{Case} + R_{Contact} = 2\frac{t_{Case}}{k_{Case} A} + \frac{R''_{Contact}}{A}. \quad (3)$$

In the considered battery grid configuration, the only varying parameter in this expression is the contact area A, as shown in Table 3.

Table 3

Parameters for thermal resistance between cells

Parameter	Symbol	Value / unit	Type	How obtained
Long-side contact area	A_{LH}	0.06885 m^2	Calculated	$A_{Length} \times A_{Height}$
Short-side contact area	A_{WH}	0.03870 m^2	Calculated	$A_{Side} \times A_{Height}$
Casing thickness	t_{case}	0.005 m	Assumed	Typical rugged battery enclosure
Casing thermal conductivity	k_{case}	0.3 W/m·K	Assumed	Typical ABS/PC plastic (0.25–0.35 W/m·K)
Area-normalized contact resistance	R"	0.001 K·m^2/W	Assumed	Typical plastic-to-plastic moderate compression

By calculating the R_{Total} for the of Valence U27-12X battery cell, it is possible to obtain 0.498 K/W for Long-side and 0.887 K/W for Short-side total thermal resistance.

5. Results of the simulation of the proposed battery management systems

5. 1. MATLAB simulation setup

5. 1. 1. High-level simulation model

To demonstrate the effectiveness of the proposed BMS controller, a battery pack model and the controller were implemented in MATLAB. The main block diagram of the simulation setup is shown in Fig. 5.

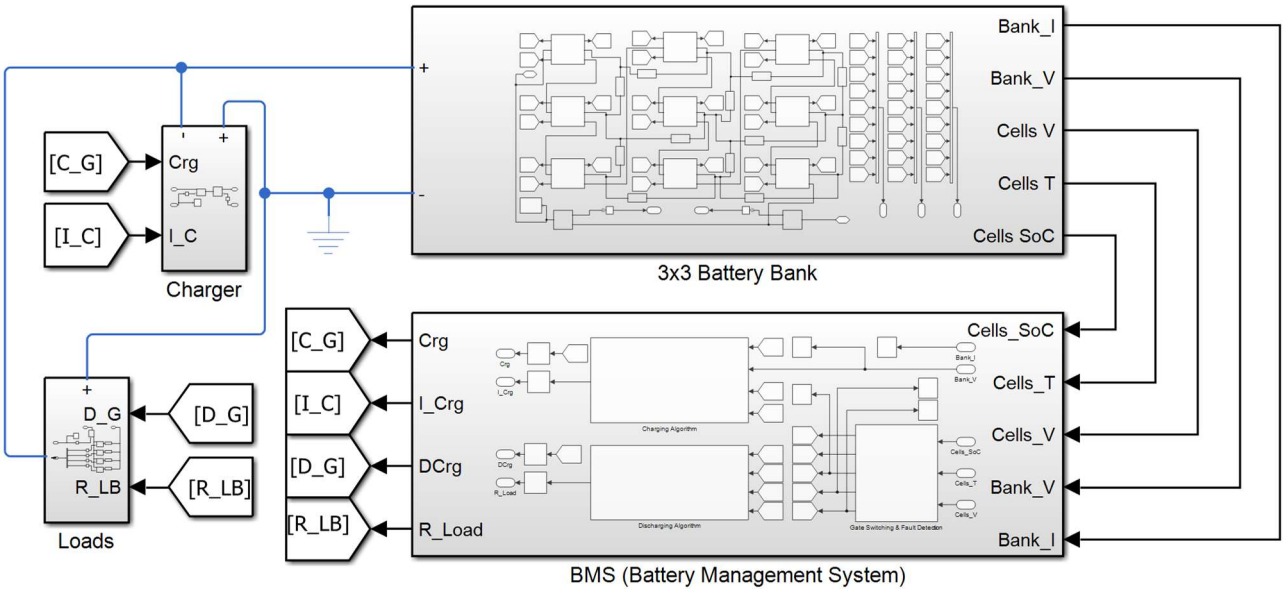

Fig. 5. General block diagram in MATLAB

The model consists of four main subsystems. The battery bank subsystem represents the batteries, with electrical connections at the terminals and outputs providing information about the state of charge, temperature, and voltage of individual cells, as well as the current through the battery bank. The BMS subsystem receives these outputs as inputs and produces control signals for the charge and discharge gates, the charger current, and the command codes used to operate the load switches.

5. 1. 2. Battery bank subsystem

The battery subsystem includes both electrical and thermal domains, shown in Fig. 6, with electrical connections in series and the thermal domain arranged in a 3×3 grid. Thermal resistances between cells use the previously established R_{total} values, applied to the long side for horizontal and the short side for vertical conduction. Each cell is modeled with a basic equivalent circuit consisting of an RC branch pair and a series internal resistance.

Each cell's subsystem is implemented using Simscape electrical and thermal blocks. Electrical behavior is represented by the battery (table-based) block, which also enables the thermal mass of the cell. The thermal mass is connected to a thermal network with convective heat transfer to represent heat exchange. For this study, the ambient temperature was set to 30°C, and the initial battery temperature was 42°C, as illustrated in Fig. 7.

The model uses the Valence U27-12XP battery from the preset options. Although all cells share the same battery parameters and ambient conditions, the convective heat transfer coefficient for each cell is determined by its placement, as the exposed surface area varies accordingly.

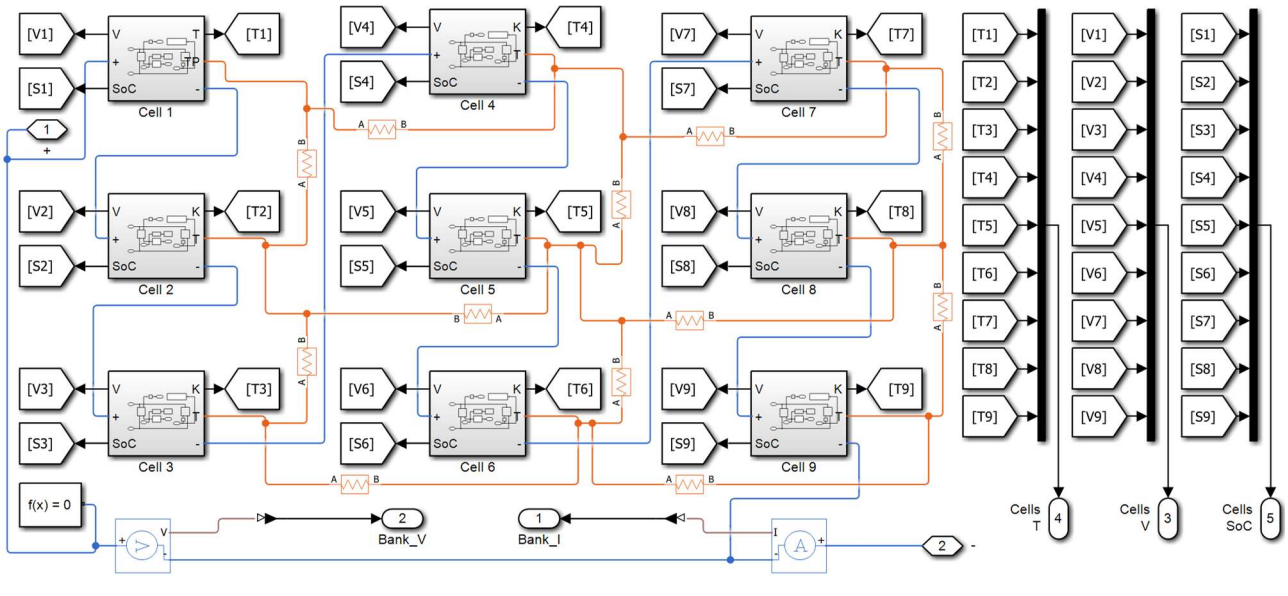

Fig. 6. Battery bank subsystem

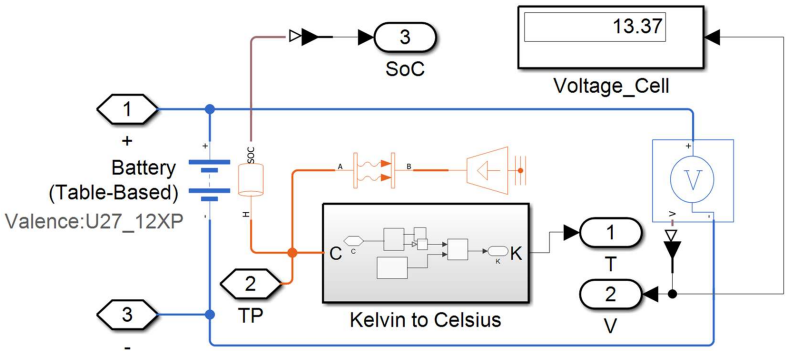

Fig. 7. Single cell subsystem

5. 1. 3. Charge subsystem

The charging subsystem is illustrated in Fig. 8. It receives the charging mode signal and the charging current as inputs. The charging mode determines whether charging is active, while the charger is modelled as a constant current source that takes the desired current as input.

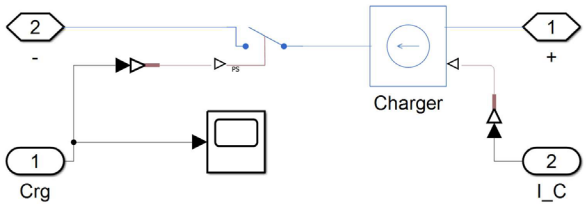

Fig. 8. Battery charging subsystem

In practice, chargers regulate current by adjusting voltage, but for this study, representing the charger as a controllable current source is sufficient and aligns with common approaches in the literature.

5. 1. 4. Discharge subsystem

The discharge subsystem, shown in Fig. 9, implements load shedding and load transfer during battery discharge. Multiple parallel loads (3.33 Ω, 5 Ω, 6.66 Ω, and 1.66 Ω) are connected with switches that determine which loads remain active and draw current from the battery.

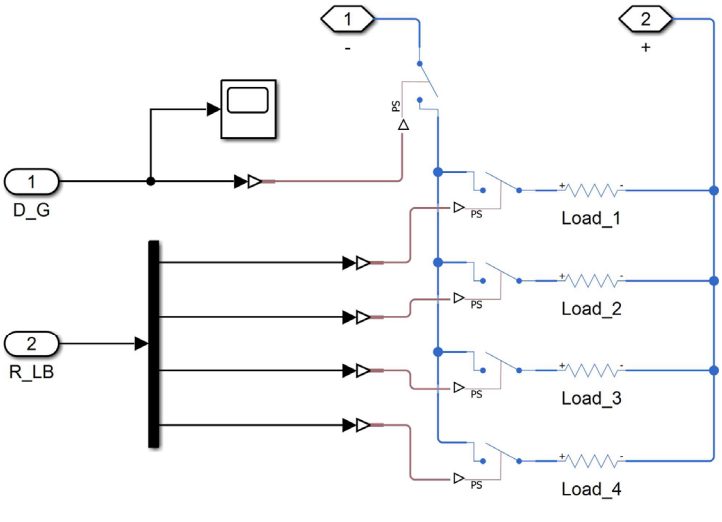

Fig. 9. Battery discharge subsystem

Although practical systems rarely consist of purely resistive loads, this simplified representation provides a closer approximation of battery behavior than the constant-current approach of the MATLAB CC-CV block. Load switch control commands are provided as a one-dimensional array and split to the corresponding gate control signals using a Demux block.

5. 1. 5. Battery management system subsystem

The BMS subsystem, which integrates both the proposed charging and discharging algorithms, is shown in Fig. 10. Its inputs include the battery bank current and voltage, as well as individual cell measurements of temperature, voltage, and state of charge (SoC). To maintain clarity, the BMS is organized into three main functional parts.

The "Gate Switching and Fault Detection" function handles whether charging or discharging is permitted based on the SoC of the cells. In addition, this block detects potential faults, such as any battery voltage falling below 75% of the battery nominal value or temperature differences exceeding 20% between any two cells. It also calculates the maximum $\frac{dT}{dt}$ temperature change rate, the maximum $\frac{dV}{dt}$ voltage change rate among all cells, and the mean temperature. The code base for this function is given below:

```
function [is_Crg, is_DCrg, T_mean, max_dT, max_dV] =
fcn(Cells_SoC, Cells_T, Cells_V)

T_mean = mean(Cells_T);
SoC_min = min(Cells_SoC);
SoC_max = max(Cells_SoC);
Fault = 0;

persistent mode % 1 = Charging -1 = Discharging
if isempty(mode)
        mode = 1; % Start in Charging Mode!
end
V_nom = 13.3;
med_T = median(Cells_T);
dev_T = abs(Cells_T - med_T) / med_T;
T_fault = any(dev_T >= 0.2);
V_fault = any(Cells_V <= 0.75 * V_nom);

Fault = T_fault || V_fault; % --- Combined fault flag

% Conflict case: one above 0.9 AND one be
% low 0.3
if (SoC_max > 0.9) && (SoC_min < 0.3) || Fault
```

```
        mode = 0; % Stop Batteries Work!

    % If currently charging and upper threshold reached →
% switch
    elseif (mode == 1) && (SoC_max > 0.9)
        mode = -1;

    % If currently discharging and lower threshold reached →
% switch
    elseif (mode == -1) && (SoC_min < 0.3)
        mode = 1;
    end

    persistent T_prev;
    if isempty(T_prev)
        T_prev = Cells_T;
    end

    dT = Cells_T - T_prev;
    max_dT = max(dT);
    T_prev = Cells_T;

    persistent V_prev;
    if isempty(V_prev)
        V_prev = Cells_V;
    end

    dV = Cells_V - V_prev;
    max_dV = max(dV);
    V_prev = Cells_V;

    if mode == 1
        is_Crg = 1;
        is_DCrg = 0;

    elseif mode == -1
        is_Crg = 0;
        is_DCrg = 1;

    else
        is_Crg = 0;
        is_DCrg = 0;
    end

    end
```

5. 2. Proposed charging algorithm

The proposed charging control algorithm for the BMS, shown in Fig. 11, regulates the charging current based on two safety considerations: cell voltage and abnormal thermal behavior. Thermal abnormalities include the cell temperature exceeding a setpoint or an unusually high temperature rise rate $\frac{dT}{dt}$ each generating an independent current reduction command.

The MATLAB implementation, presented in Fig. 12, receives the battery bank current and voltage, mean cell temperature, and charging mode as inputs. It calculates individual scaling factors in the range [0, 1] for voltage regulation, temperature overheating, and rapid temperature increase. The final charging current command is obtained by multiplying the most restrictive scaling factor to the reference maximum charger current.

One current reduction branch uses the Battery CC-CV block to regulate charging based on the battery bank voltage. The block receives the measured current and voltage and adjusts the charging current as the voltage approaches the predefined limit, operating in either constant-current (CC) or constant-voltage (CV) mode. For this study, CC-CV block was set with voltage threshold of 121V, proportional gain of 3.33 and integral gain of 0.33 with other parameters remaining as default. This branch is enabled only during charging, while discharging is handled separately through load shedding. To address thermal dynamics, two fuzzy logic controllers (FLCs) provide additional current reduction branches. One monitors the temperature control error, and the other evaluates the temperature rise rate $\frac{dT}{dt}$, generating reduction factors that are later compared with other control branches to determine the final charging current.

The first FLC regulates charging based on the temperature control error, defined as the difference between the measured mean cell temperature and the setpoint. Input and output membership functions are in range from 0 to 1 (Tables 4, 5), with the corresponding rule base in Table 6. When the error is between −1 and −0.5, only a mild current reduction of up to 10% is applied. As the error approaches 0, the reduction increases gradually to ensure a smooth transition, while positive errors trigger more aggressive reductions up to 100%, providing fast corrective action while maintaining stable approach behavior toward the setpoint.

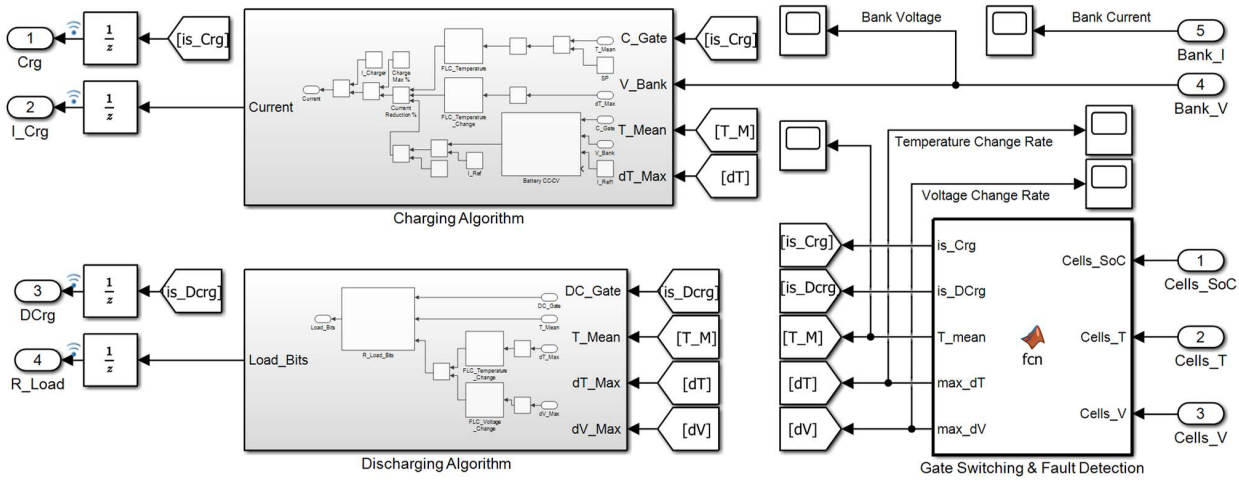

Fig. 10. Battery management system controller subsystem

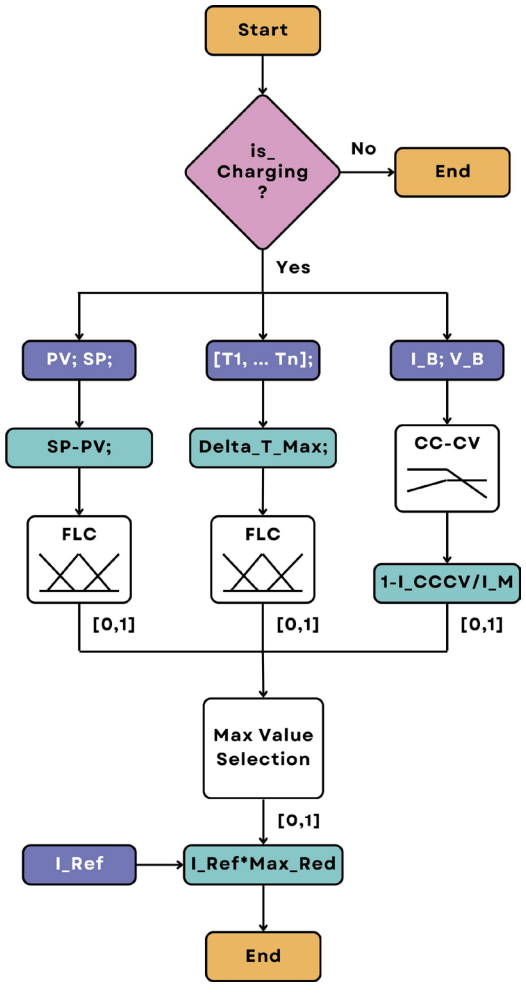

Fig. 11. Battery charging control system algorithm

The second FLC monitors the temperature rise rate, adding protection against rapid thermal transients. Its membership functions are in range from 0 to 1 for its output and from 0.01 to 0.05 for its input (Tables 7, 8), with the rule base in Table 9. The controller is triggered only when the rise rate exceeds 0.01°C per sampling interval, establishing a minimum threshold to ensure normal battery operation does not unnecessarily reduce the charging current. Its action increases as the rate approaches 0.05°C to prevent thermal escalation.

Table 4

Charge control error fuzzy logic controller input

Name	Type	Value
Low	Triangular fuzzy number	[0, 0, 0.4166]
Medium	Triangular fuzzy number	[0.0833, 0.5, 0.9166]
High	Triangular fuzzy number	[0.5833, 1, 1]

Table 5

Charge control error fuzzy logic controller output

Name	Type	Value
Low	Real number	0
Medium	Real number	0.1
High	Real number	1

Table 6

Charge control error fuzzy logic controller rule table

Number	Rule	Weight	Name
1	If control error is low then current reduction is high	1	Rule 1
2	If control error is medium then current reduction is medium	1	Rule 2
3	If control error is high then current reduction is low	1	Rule 3

In the present simulation, this threshold is not exceeded, but the limits ensure the system can respond effectively under transient or non-ideal conditions.

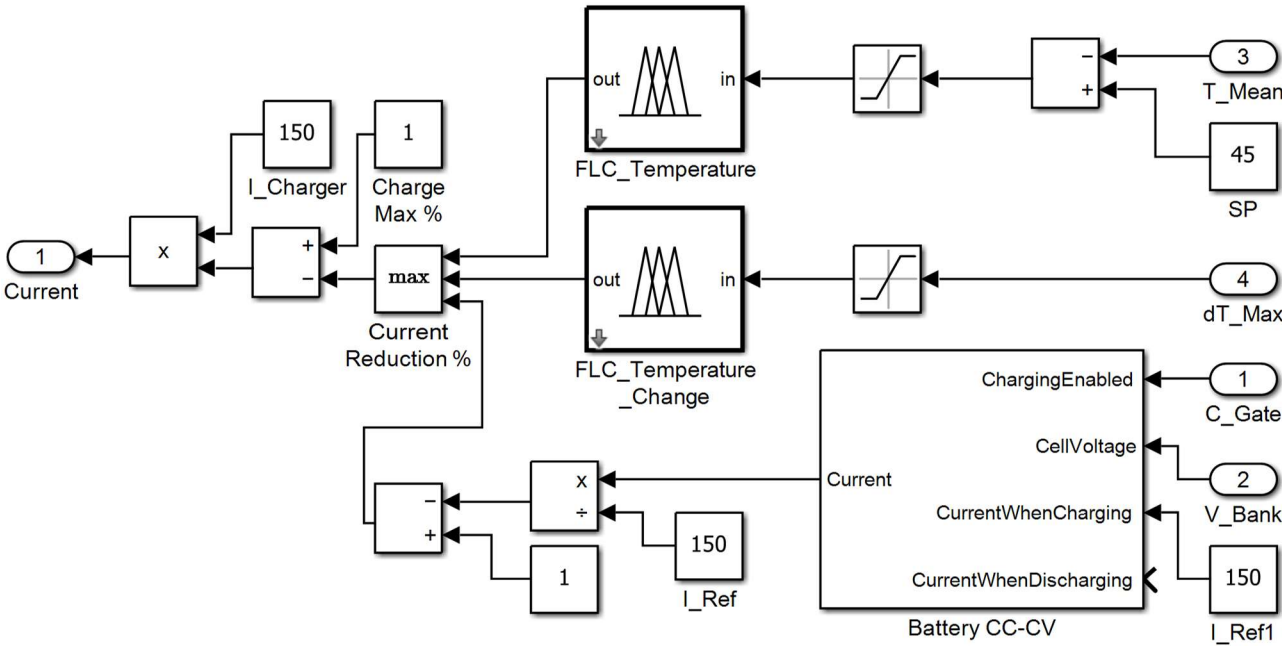

Fig. 12. Battery charging control system algorithm subsystem

Table 7

Charge temperature change (Delta T) Fuzzy Logic controller input

Name	Type	Value
Low	Triangular fuzzy number	[0.01, 0.01, 0.0266]
Medium	Triangular fuzzy number	[0.0133, 0.03, 0.0466]
High	Triangular fuzzy number	[0.0333, 0.05, 0.05]

Table 8

Charge temperature change (Delta T) Fuzzy Logic controller output

Name	Type	Value
Low	Real number	0
Medium	Real number	0.5
High	Real number	1

Table 9

Charge temperature change (Delta T) Fuzzy Logic controller rule table

Number	Rule	Weight	Name
1	If Delta T is low then current reduction is low	1	Rule 1
2	If Delta T is medium then current reduction is medium	1	Rule 2
3	If Delta T is high then current reduction is high	1	Rule 3

5. 3. Proposed discharge algorithm

In Fig. 13, the proposed algorithm for managing current regulation in battery management system (BMS) is shown. The algorithm relies on a mapped array of load configurations to determine how loads should be shed or transferred. Its main goal is to identify when to shift the array index up or down to adjust the active loads. The discharge algorithm first evaluates the outputs of two FLCs, monitoring voltage drop $\frac{dV}{dt}$ and temperature rise $\frac{dT}{dt}$, to determine whether a rapid bypass load reduction is required. The system checks if the battery is actively discharging. Persistent variables track the previous discharge mode to detect a recent swap from charge to discharge, triggering a three-step change delay. If the change delay is active, all further load adjustments are skipped. Otherwise, the algorithm applies the following sequence. If the bypass reduction from the FLCs is nonzero, it is applied immediately. Else, if the temperature exceeds the setpoint, loads are reduced only when T_{max} consistently increases, and the change delay is triggered. Else if the temperature is below the setpoint minus a hysteresis margin, loads may be added back, also triggering the change delay. In all other cases, the load configuration remains unchanged. Finally, previous voltage gates are updated, load commands are executed, and any active change delay is decremented.

Fig. 14 shows the implementation of this algorithm in MATLAB. The inputs include the discharge mode, the mean cell temperature, the maximum temperature rise $\frac{dT}{dt}$, and the maximum voltage drop $\frac{dV}{dt}$ of an individual cell.

A dedicated FLC is introduced to evaluate the voltage drop rate, defined over a range from −0.002 to −0.001 V per sampling interval, representing the safe operating region. More negative values indicate potentially critical conditions and result in increased current reduction. Under the ideal conditions of the present simulation, such behavior is difficult to trigger without altering these thresholds beyond their intended physical meaning. Therefore, the controller is included primarily to illustrate the control approach, with its input and output membership functions given in Tables 10, 11, and the rule base in Table 12.

Table 10

Voltage change (Delta V) fuzzy logic controller input

Name	Type	Value
Low	Triangular fuzzy number	[–0.002, –0.002, –0.001583]
Medium	Triangular fuzzy number	[–0.001916, –0.0015, –0.001083]
High	Triangular fuzzy number	[–0.001416, –0.001, –0.001]

Table 11

Voltage change (Delta V) fuzzy logic controller output

Name	Type	Value
Low	Real number	0
Medium	Real number	0.5
High	Real number	1

Table 12

Voltage change (Delta V) fuzzy logic controller rule table

Number	Rule	Weight	Name
1	If Delta V is low then shed count is high	1	Rule 1
2	If Delta V is medium then shed count is medium	1	Rule 2
3	If Delta V is high then shed count is low	1	Rule 3

Another dedicated FLC is introduced to evaluate the temperature rise rate. Its input range is identical to that used in the charging temperature rise rate FLC, as shown in Table 13. The key difference lies in the output, which in this case determines the number of loads to be shed, as presented in Table 14. The rule base follows a similar trend to the charging FLC, as shown in Table 15, applying stronger load reduction as the temperature rise becomes more significant.

Table 13

Discharge temperature change (Delta T) fuzzy logic controller input

Name	Type	Value
Low	Triangular fuzzy number	[0.01, 0.01, 0.0266]
Medium	Triangular fuzzy number	[0.0133, 0.03, 0.0466]
High	Triangular fuzzy number	[0.0333, 0.05, 0.05]

Table 14

Discharge temperature change (Delta T) fuzzy logic controller output

Name	Type	Value
Low	Real number	0
Medium	Real number	3
High	Real number	5

Table 15

Discharge temperature change (Delta T) fuzzy logic controller rule table

Number	Rule	Weight	Name
1	If Delta T is low then load reduction is low	1	Rule 1
2	If Delta T is medium then load reduction is medium	1	Rule 2
3	If Delta T is high then load reduction is high	1	Rule 3

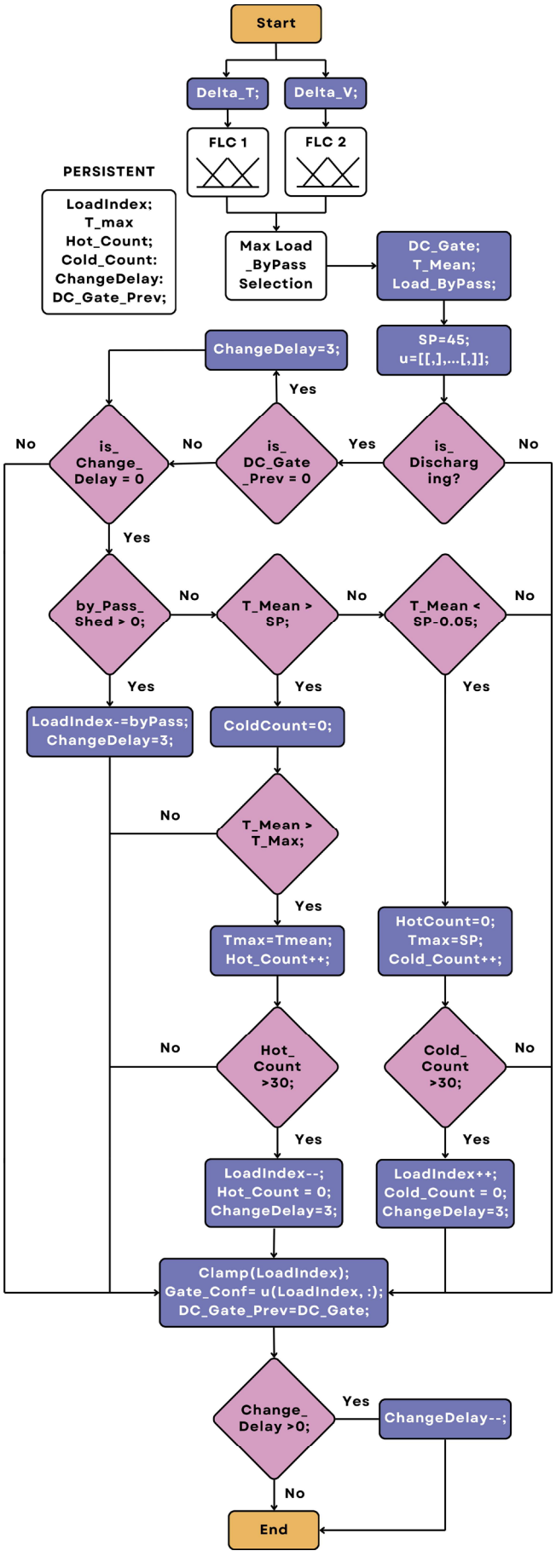

Fig. 13. Load shedding control system algorithm

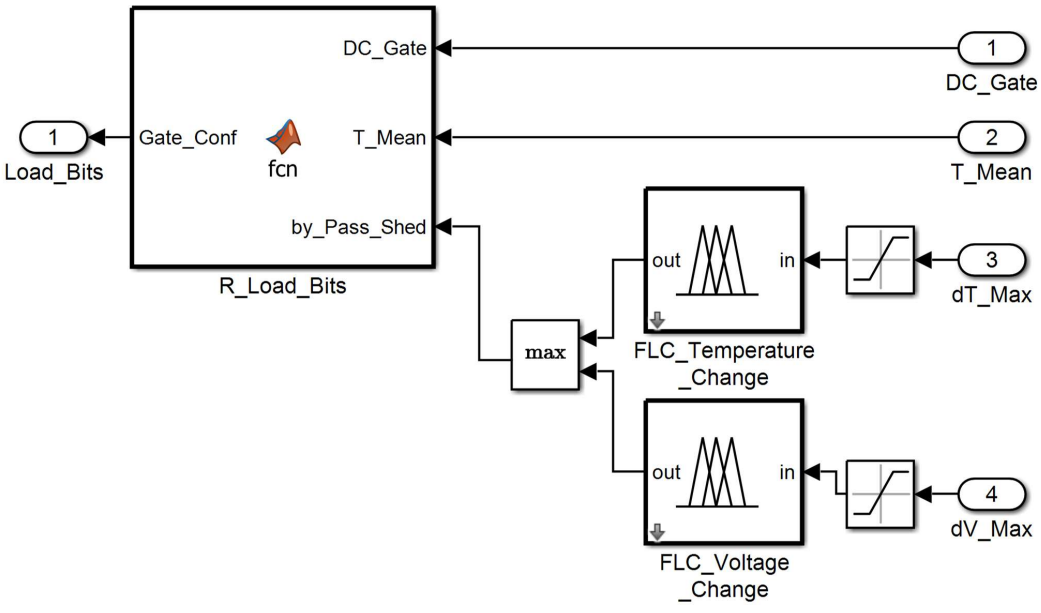

Fig. 14. Load shedding control system algorithm subsystem

Dynamically determining the correct order of load configurations from highest to lowest current can become computationally expensive during runtime. To address this, a predefined, order-based mapping can be used to ensure the correct load sequence regardless of the number of bits, facilitating efficient load management during discharge:

```
V = 120;              % Total Voltage (V_Total)
R = [R_1, ... R_n];       % Resistances (Ohm)
I = V./R;             % Individual Currents

fprintf('Individual currents (A):\n')
fprintf('R%d = %g Ohm -> I%d = %.2f A\n', [1:N;R;1:N;I])
fprintf('\n')

B = dec2bin(0:2^n-1)-'0';       % Binary States
T = B*I.';                % Total Current

disp('Unsorted combinations:')
disp(array2table([B  T],'VariableNames',{'B1' ... 'Bn','
TotalCurrent_A'}))

[Ts,idx] = sort(T);
Bs = B(idx,:);
disp('Sorted combinations (Ascending Current):')
disp(array2table([Bs  Ts],'VariableNames',{'B1' ... 'Bn','
TotalCurrent_A'}))

fprintf('\nFinal Check:\nMin: %.2f A\nMax: %.2f
A\n',Ts(1),Ts(end))
```

Table 16 presents the results for a four-load configuration mapping for scaled maximum 50A current flow, illustrating the applied order and corresponding current distribution. Once it is possible to obtain the mapped binary index array of the load gates, it is possible to integrate load shedding mechanism based on cells mean temperature reading.

The proposed discharge algorithm MATLAB Function block is listed below:

```
functionGate_Conf=fcn(DC_Gate,T_Mean,by_Pass_Shed)

SP = 45;
u = [0,0,0,0; 0,0,1,0; 0,1,0,0; 1,0,0,0;
    0,1,1,0; 1,0,1,0; 1,1,0,0; 0,0,0,1;
    1,1,1,0; 0,0,1,1; 0,1,0,1; 1,0,0,1;
    0,1,1,1; 1,0,1,1; 1,1,0,1; 1,1,1,1];

persistent LoadIndex Tmax HotCount ColdCount
ChangeDelay DC_Gate_Prev
if isempty(LoadIndex)
    LoadIndex = 16;
    Tmax = SP;
    HotCount = 0;
    ColdCount = 0;
    ChangeDelay = 0;
    DC_Gate_Prev = DC_Gate;
end
if DC_Gate == 1% ---- MAIN CONTROL ----

    if DC_Gate_Prev == 0
        ChangeDelay = 3;
    end

    if ChangeDelay == 0
        by_Pass_Shed = by_Pass_Shed - mod(by_Pass_
Shed, 1);
        if by_Pass_Shed > 0% ---- BYPASS LOAD SHED-
DING ----
            LoadIndex = LoadIndex - by_Pass_Shed;
            ChangeDelay = 3;

        elseif T_Mean > SP % -------- HOT CASE --------
            ColdCount = 0;
            if T_Mean >= Tmax
                Tmax = T_Mean;
                HotCount = HotCount + 1;

                if HotCount >= 30
                    LoadIndex = LoadIndex - 1;
                    HotCount = 0;
```

```
                ChangeDelay = 3;
            end
        end

    elseif T_Mean < SP-0.05% -------- COLD CASE --------
        Tmax = SP;
        ColdCount = ColdCount + 1;
        HotCount = 0;
        if ColdCount > 30
            LoadIndex = LoadIndex + 1;
            ColdCount = 0;
            ChangeDelay = 3;
        end
    end
  end
end

LoadIndex = max(1, min(16, LoadIndex));
Gate_Conf = u(LoadIndex, :);
DC_Gate_Prev = DC_Gate;
if ChangeDelay > 0
  ChangeDelay = ChangeDelay - 1;
end

end
```

Table 16

Load mapping for $R = [10, 15, 20, 5]$ configuration, where $A = [12, 8, 6, 24]$

Order	Unsorted		Sorted		Order	Unsorted		Sorted	
	Bits	Current	Bits	Current		Bits	Current	Bits	Current
0	0000	0	0000	0	8	1000	12	1110	26
1	0001	24	0010	6	9	1001	36	0011	30
2	0010	6	0100	8	10	1010	18	0101	32
3	0011	30	1000	12	11	1011	42	1001	36
4	0100	8	0110	14	12	1100	20	0111	38
5	0101	32	1010	18	13	1101	44	1011	42
6	0110	14	1100	20	14	1110	26	1101	44
7	0111	38	0001	24	15	1111	50	1111	50

5. 4. Simulation results for evaluation of effectiveness in current regulation and temperature stabilization

The current response in Fig. 15 shows the dynamic behavior of the battery system. In this plot it is possible to observe three cycles. During the initial charge cycle, the current started at −150 A in charging mode and gradually changed to around −95 A before transitioning to discharge mode. During discharge cycle, the current initially spiked to 143.85 A and then reduced through load shedding with some fluctuations before stabilizing at around 102.5 A. Finally, during the last charge cycle current initially dropped to 0 A and then gradually stabilized around −104 A. This behavior reflects the coordinated operation of the charging and discharging control strategies.

Further analysis of battery bank voltage in Fig. 16 shows how voltage changed throughout these stages. During the initial charge mode, the terminal voltage went above the CC-CV blocks voltage threshold of 121 V, thus PID action was triggered which explaining the initial current change from −150 A to around −95 A in Fig. 15. Afterwards during the next discharge and charge cycles the voltage remained under 121 V threshold. However, an important observation here is to note that voltage can drop significantly during load sheds and charge-discharge cycle changes.

The temperature plot in Fig. 17 shows that the use of two different approaches for charge and discharge is effective at keeping temperature below the setpoint (SP). During the first charge cycle, the temperature initially started as 42°C and remained below the SP of 45°C. During the following discharge cycle, load shedding or transferring action had to be made to prevent temperature from reaching the SP, which explains current fluctuations in Fig. 15. Finally, during final charging cycle, the temperature remained below SP with small undershoot due to FLC design.

In Fig. 18, the plot diagram of temperature change rate is shown. The main concern with temperature is to keep track of any rapid temperature rise trends, as they are the main indicator of thermal runaways, faulty, and aging batteries. However, since this is an ideal simulation, such behavior is hard to replicated in such conditions. But nevertheless, they are worth mentioning.

In Fig. 19, the plot diagram of rate of change of the voltage is shown. The main concern with voltage monitoring is the trend of rapid voltage drops. For this reason, it is mainly possible to focus on any sharp spikes below zero. In our case, it is possible to observe these spikes mainly for two reasons during changing from charging to discharging and when load is added back.

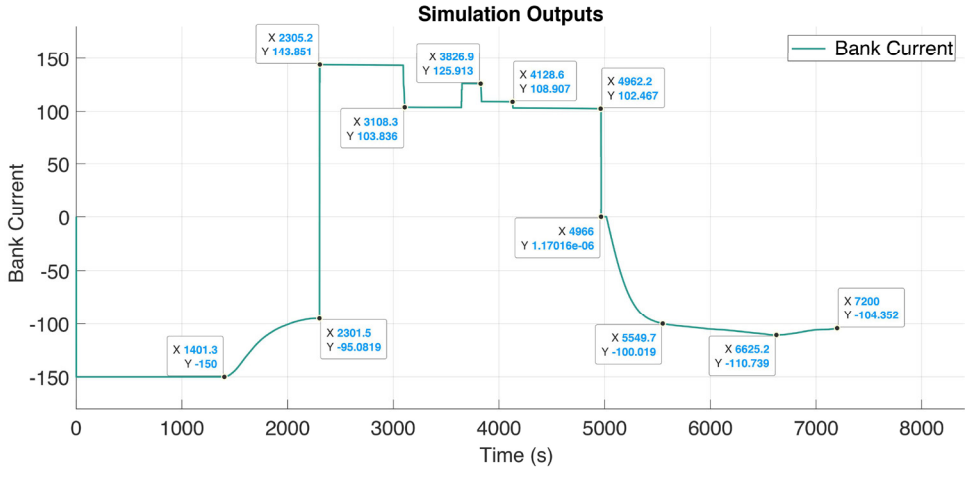

Fig. 15. Plot of battery bank current

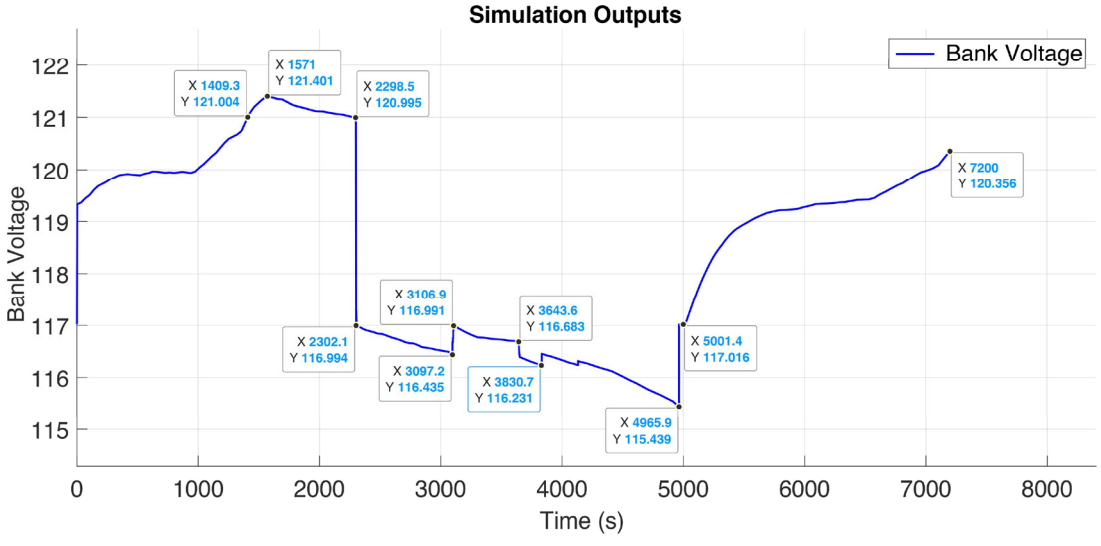

Fig. 16. Plot of battery bank voltage

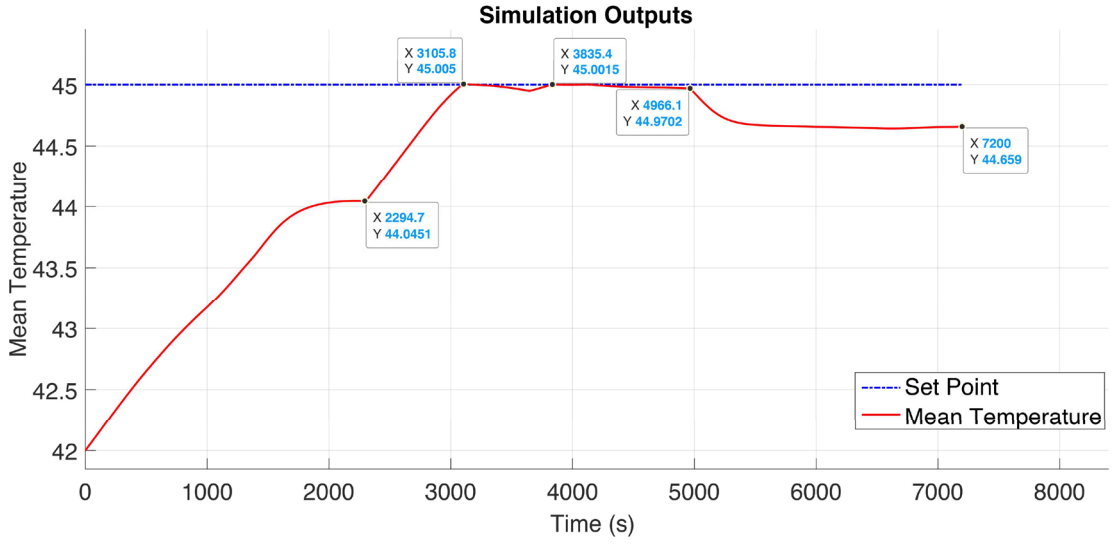

Fig. 17. Plot of mean temperature of battery cells

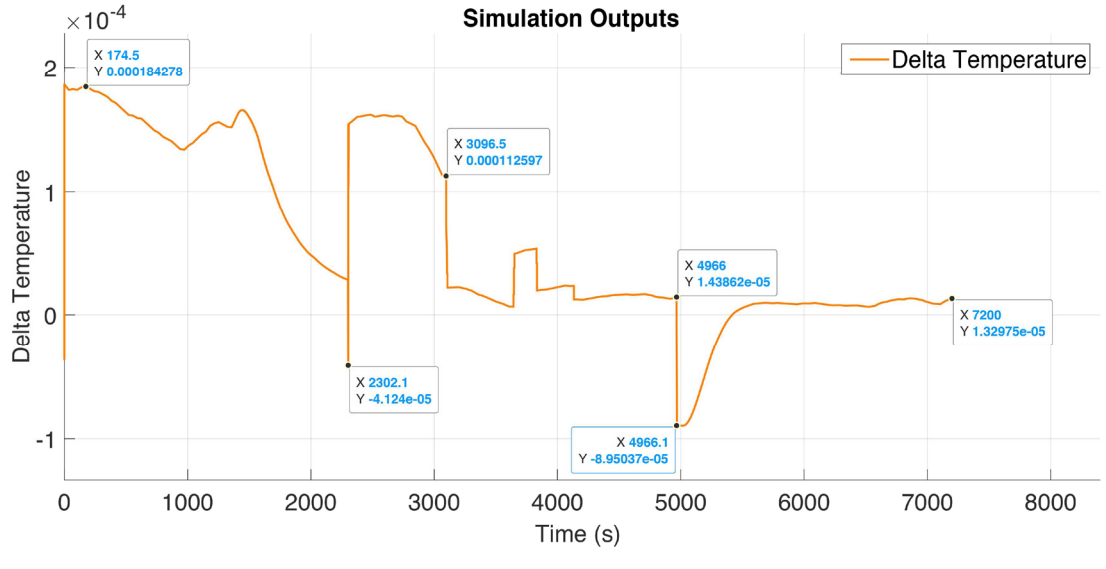

Fig. 18. Plot of maximum rate of temperature change among all cells

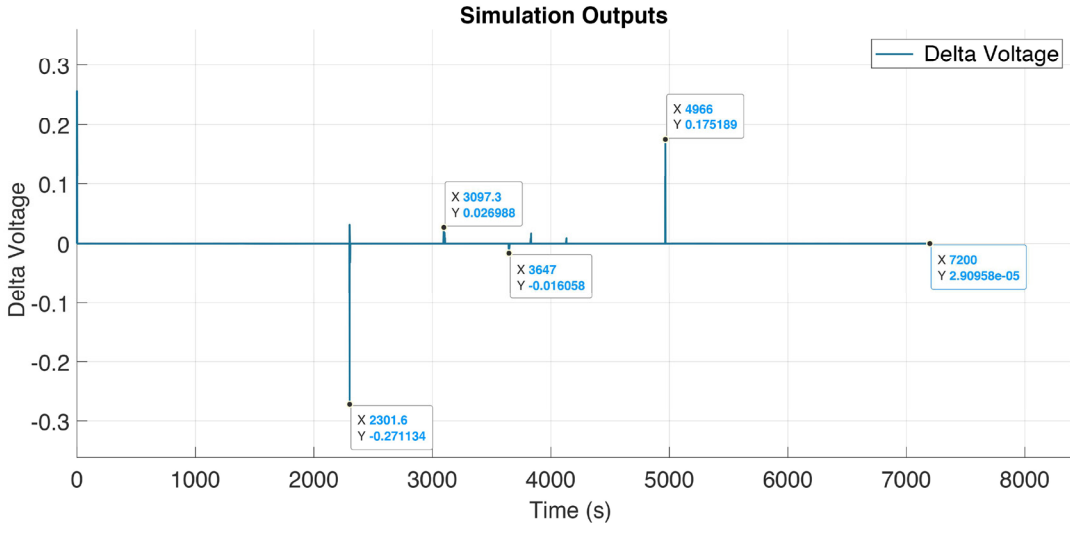

Fig. 19. Plot of maximum rate of voltage change among all cells

However, since neither of these voltage drops are truly faulty behavior, the controller design for the proposed shedding or transferring was set to account for this. In addition to this, similar to sudden temperature rise, the sudden voltage drops under faulty operation are also hard to replicate during ideal simulation conditions.

6. Discussion of results for proposed battery management systems

The results of this study provide the importance of the study's problem and align with the study's aim and objectives. This obtained within the framework of our study are explained with the 3 charge-discharge cycle resulting from the proposed charge-discharge strategy which combined two complementary mechanisms:

– during the initial charge cycle, it is possible to observe that in Fig. 16 voltage overshoot above its 121V setpoint in the CC-CV block around time step 1409 which resulted in gradual current drop from -150 A to around -95 A in Fig. 15 staring from time step of around 1401. This cycle lasted till time step 2301 as can be seen by the current change in the Fig. 15 around the same step. During this initial charging cycle, temperature remained below its set point, reaching a peak of approximate 44°C at time step 2294 as shown in Fig. 17;

– during the following discharge cycle the temperature exceeded the setpoint around step 3105 as shown in Fig. 17, which triggered load shedding or transferring resulting in sudden current drops as observed in the Fig. 15 around the same step. After the initial one, few more load shedding and transferring actions took place to balance the temperature during time steps of around 3097, 3643 and 3830. These fluctuations are most clearly visible in the voltage graph in Fig. 16 around the same time steps. These load shedding and transferring actions were performed to stabilize the temperature as can be seen in Fig. 17, where temperature remained in very close proximity of the setpoint throughout the discharge cycle from time steps around 3105 to roughly time step 4966 where terminal voltage in Fig. 16 reached its lowest point of around 115.4 V. It is also worth to mention that sudden voltage changes occurred during both the start and the end of this discharge cycle as seen in Fig. 19;

– finally, during the last charge period, the temperature was already near the setpoint as can be seen in Fig. 17. This resulted in current flow in Fig. 15 to gradually recover to prevent overshooting in the temperature setpoint starting from around time step 4966. As current plot in Fig. 15 shows that initial no current was flowing at that time step due to temperature being at close proximity to the set point in Fig. 17. However, gradually the current flow recovered to around –104 A around time step of 5550 till 7200 as shown in Fig. 15, while the temperature also recovered to its steady state of 44.65°C around the same time step as shown in Fig. 17. The final steady state value due to the FLC design in Table 4, which reduces current rapidly once it exceeds 44°C and stops it completely as it gets closer to 45°C to prevent overshoot.

From the results it is possible to observe that, by using the proposed controller to adjust the current during charging and discharging as illustrated in Fig. 15, the system maintained stable voltage and temperature throughout the entire simulation duration as plotted in Fig. 16, 17.

The advantages of the proposed battery management systems are as follows:

– the proposed method accounts for separate discharging control strategy, which makes it fundamentally different from the fast charge algorithm works, typical of [2] and their modifications with other algorithms [1];

– during unsafe behavior like sudden voltage drop or temperature rise, the load is automatically transferred or shed. This effect is absent in studies like [7];

– this work regulates both charging and discharging current, compare to some existing works such as development of balancing strategy [8] and predicting temperature [6];

– the temperature is accounted for as a key parameter compare to previous works which implemented separate charge and discharge strategies [10];

– the discharge strategy accounts for real life discharge challenges by taking load shedding or transferring into account [13, 14].

The solution obtained by using MATLAB simulation confirmed the battery temperature and voltage prediction helps to control the battery charging and discharging current as shown in Fig. 16.

The main limitation of this study is the ideal scenario-based simulation, which does not account of battery aging,

degradation or thermal runaway cases. Another limitation is the only current regulation consideration, but in practical applications there are usually additional cooling and heating mechanisms [9].

The main disadvantage of this strategy is the complexity of its design. Another issue to consider is the sensor inaccuracies or single point failures which might trick the discharge algorithm to trigger load shedding or minimize charging current by mistakenly and it is possible to encounter power outage for critical loads or less energy storage.

The difficulties for implementing this controller strategy are additional equipment and software requirement. In addition to this, load shedding and transferring will require additional available battery to allocate the shredded loads.

7. Conclusion

1. The simulation environment enables a detailed representation of both electrical and thermal dynamics of each battery. The advanced modelling captures charging and discharging behavior and the interaction between current and temperature.

2. The controller for charging mechanism uses both the CC–CV and fuzzy-based temperature error and temperature rise rate evaluation mechanisms to choose the most critical parameter to reduce the current by. The application of fuzzy logic in this approach are easy to design, while also preventing overshoot and maintaining reliability under varying operation conditions during charging.

3. The controller for the discharge mechanism consist of pre-mapped load configuration with fuzzy decision-making system for load shedding and load transferring. This algorithm ensures stable operation during discharge cycle. This algorithm also considers the false load shedding and load transferring scenarios.

4. The effectiveness of the proposed advanced control strategies was validated through simulation results of 7200-time steps, demonstrating controlled current profiles during two charging and one discharging cycle. The system maintains the temperature below the setpoint of 45°C and responds effectively to changing conditions.

Conflict of interest

The authors declare that they have no conflict of interest in relation to this study, whether financial, personal, authorship or otherwise, that could affect the study and its results presented in this paper.

Financing

The study was performed without financial support.

Data availability

Manuscript has no associated data.

Use of artificial intelligence

The authors confirm that they did not use artificial intelligence technologies in creating the submitted work.

Authors' contributions

Rahim Mammadzada: Conceptualization, Methodology, Software, Validation, Formal analysis, Investigation, Data Curation, Writing – original draft, Writing – review & editing, Visualization; **Ruslan Mammadov**: Conceptualization, Methodology, Validation, Formal analysis, Investigation, Resources, Writing – original draft, Writing – review & editing, Supervision, Project administration.

References

1. Károlyi, G., Pózna, A. I., Hangos, K. M., Magyar, A. (2022). An Optimized Fuzzy Controlled Charging System for Lithium-Ion Batteries Using a Genetic Algorithm. Energies, 15 (2), 481. https://doi.org/10.3390/en15020481
2. Shaout, A. K., Brauchler, Z. (2025). Fuzzy Battery Manager: Charging and Balancing Rechargeable Battery Cells with Fuzzy Logic. Electronics, 14 (7), 1470. https://doi.org/10.3390/electronics14071470
3. Mammadzada, R. (2025). System-Level Conceptual Analysis of Thermal Behavior in Solar Microgrids with Fuzzy Logic Perspective. Journal of Modern Technology and Engineering, 10 (3). https://doi.org/10.62476/jmte.103141
4. Behera, S., Dev Choudhury, N. B. (2024). Optimal battery management in PV + WT micro-grid using MSMA on fuzzy-PID controller: a real-time study. Sustainable Energy Research, 11 (1). https://doi.org/10.1186/s40807-024-00136-w
5. Xiong, R., Zhao, Z., Chen, C., Li, X., Shen, W. (2024). Electrothermal Model Based Remaining Charging Time Prediction of Lithium-Ion Batteries against Wide Temperature Range. Chinese Journal of Mechanical Engineering, 37 (1). https://doi.org/10.1186/s10033-024-01024-6
6. Zhang, H., Fotouhi, A., Auger, D. J., Lowe, M. (2024). Battery Temperature Prediction Using an Adaptive Neuro-Fuzzy Inference System. Batteries, 10 (3), 85. https://doi.org/10.3390/batteries10030085
7. Acker, L., Hofmann, P., Konrad, J. (2025). Predictive battery thermal management for fast charging of electric vehicles using nonlinear model predictive control and dynamic programming. Automotive and Engine Technology, 11 (1). https://doi.org/10.1007/s41104-025-00157-7
8. Su, X., Zou, G., An, S., Zou, H., Wang, X. (2025). Research on Equalization Strategy of Lithium-Ion Battery Based on Temperature and SOC Adaptive Fuzzy Control. Energies, 18 (3), 581. https://doi.org/10.3390/en18030581
9. Zhang, S., Li, T., Chen, L. (2023). Fuzzy Logic Control of External Heating System for Electric Vehicle Batteries at Low Temperature. World Electric Vehicle Journal, 14 (4), 99. https://doi.org/10.3390/wevj14040099

10. Goksu, O. F., Arabul, A. Y., Acar Vural, R. (2020). Low Voltage Battery Management System with Internal Adaptive Charger and Fuzzy Logic Controller. Energies, 13 (9), 2221. https://doi.org/10.3390/en13092221
11. Zadeh, L. A. (1965). Fuzzy sets. Information and Control, 8 (3), 338–353. https://doi.org/10.1016/s0019-9958(65)90241-x
12. Mammadzada, R. (2025). Performance Evaluation of PID and Fuzzy Logic Control Strategies Under Charge-Discharge Cycles in a Simscape-Based Thermal-Electrical Battery System. Journal of Modern Technology and Engineering, 10 (3). https://doi.org/10.62476/jmte.103213
13. Mammadov, R., Yusubov, E. (2025). Metaheuristic Load Shedding Method Using Binary Decision Variables for Controllable Loads. 2025 5th International Conference on Electrical, Computer and Energy Technologies (ICECET), 1–6. https://doi.org/10.1109/icecet63943.2025.11472308
14. Mammadov, R. (2025). Optimal Load Shedding for Power Systems Using the Binary Exhaustive Search Method. Intelligent and Fuzzy Systems, 175–183. https://doi.org/10.1007/978-3-031-98304-7_20